© 2000 Nature America Inc. • http://genetics.nature.com

Impaired insulin secretion and β-cell loss in tissue-specific knockout mice with mitochondrial diabetes

José P. Silva[1], Martin Köhler[2], Caroline Graff[1], Anders Oldfors[3], Mark A. Magnuson[4], Per-Olof Berggren[2] & Nils-Göran Larsson[1]

Mitochondrial dysfunction is an important contributor to human pathology[1–4] and it is estimated that mutations of mitochondrial DNA (mtDNA) cause approximately 0.5–1% of all types of diabetes mellitus[5,6]. We have generated a mouse model for mitochondrial diabetes by tissue-specific disruption of the nuclear gene encoding mitochondrial transcription factor A (Tfam, previously mtTFA; ref. 7) in pancreatic β-cells. This transcriptional activator is imported to mitochondria, where it is essential for mtDNA expression and maintenance[8,9]. The *Tfam*-mutant mice developed diabetes from the age of approximately 5 weeks and displayed severe mtDNA depletion, deficient oxidative phosphorylation and abnormal appearing mitochondria in islets at the ages of 7–9 weeks. We performed physiological studies of β-cell stimulus–secretion coupling in islets isolated from 7–9-week-old mutant mice and found reduced hyperpolarization of the mitochondrial membrane potential, impaired Ca^{2+}-signalling and lowered insulin release in response to glucose stimulation. We observed reduced β-cell mass in older mutants. Our findings identify two phases in the pathogenesis of mitochondrial diabetes; mutant β-cells initially display reduced stimulus–secretion coupling, later followed by β-cell loss. This animal model reproduces the β-cell pathology of human mitochondrial diabetes and provides genetic evidence for a critical role of the respiratory chain in insulin secretion.

We have determined the consequences of loss of mtDNA expression in mouse pancreatic β-cells by tissue-specific disruption of *Tfam*. We mated mice with a *loxP*-flanked *Tfam* allele (*Tfam*^{tm1Lrsn}, hereafter *Tfam*^{loxP}; refs 8,9) to transgenic mice with *cre*-recombinase expression regulated by the rat insulin-2 promoter (TgN(ins2-*cre*)25Mgn or *RIP-cre*; refs 10–12). The resulting mice were homozygous for *Tfam*^{loxP} and heterozygous for *RIP-cre* (*Tfam*$^{tm1.4Lrsn}$, hereafter *Tfam*^{loxP}/*Tfam*^{loxP}, +/*RIP-cre*). We studied the tissue specificity of these mice by PCR analyses and found the mutant allele (*Tfam*$^{-}$) in pancreas and brain in 7-week mutant mice (Fig. 1*a*) and in only brain in 14- and 27–39-week mutant mice (data not shown).

We used *in situ* hybridization to study the distribution of mtDNA in the pancreas and found severe mtDNA depletion in islets of mutant mice at 7 weeks (Fig. 1*b*). We next determined the respiratory chain function in pancreas by enzyme histochemical double staining for cytochrome *c* oxidase (COX) and succinate dehydrogenase (SDH) activities. We observed severe COX deficiency and normal SDH activity in islets of mutant mice at 7 weeks (Fig. 1*b*). This result is expected because COX contains mtDNA-encoded catalytic subunits, whereas SDH is exclusively nucleus-encoded. Electron microscopy of pancreatic sections revealed abundant abnormally appearing mitochondria with tubular

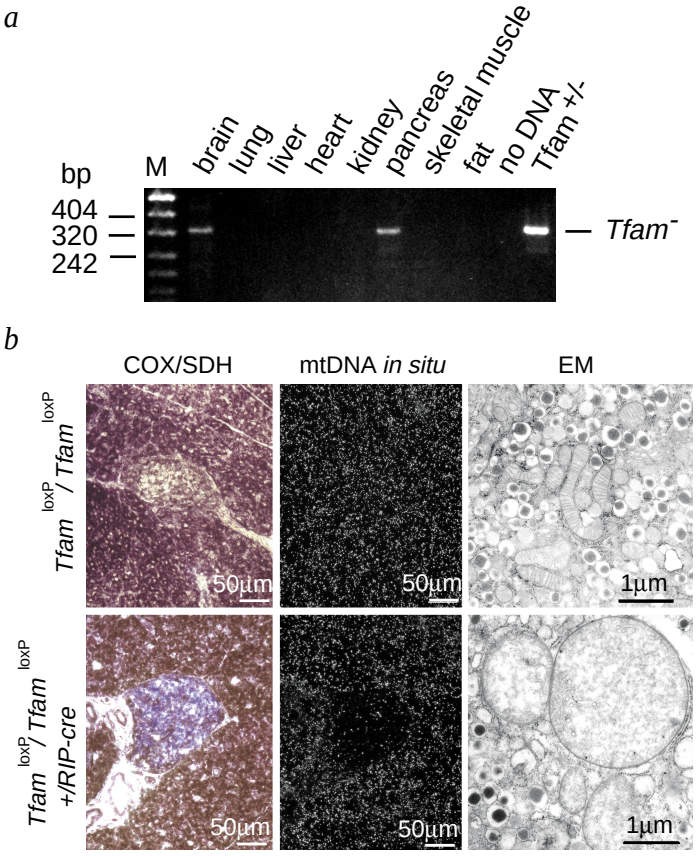

Fig. 1 Genotyping of different tissues in mutant mice (*Tfam*^{loxP}/*Tfam*^{loxP}, +/*RIP-cre*) and morphological studies of pancreas in mutant mice and controls (*Tfam*^{loxP}/*Tfam*^{loxP}). ***a***, PCR analyses to detect the knockout allele (*Tfam*$^{-}$) in a 7-week mutant mouse. The lane indicated M shows a molecular weight marker. The other lanes show the results from PCR analyses of DNA from different organs from the mutant, a negative control sample without DNA (no DNA) and positive control sample with DNA from a germ line heterozygous knockout mouse (*Tfam*$^{+/-}$). ***b***, Enzyme histochemical double staining for cytochrome *c* oxidase (COX) activity and succinate dehydrogenase (SDH) activity (left), *in situ* hybridization to detect mtDNA (middle) and electron micrographs (EM; right) of islets of mutant mice and littermate controls at the age of 7 weeks. The serial sections (*b*, left and middle) show extensive COX deficiency, as indicated by the blue staining, and mtDNA depletion in islets from mutant mice. The EM shows abnormally enlarged mitochondria with tubular cristae in a β-cell from a mutant islet.

[1]*Department of Molecular Medicine, Karolinska Institutet, Karolinska Hospital, Stockholm, Sweden.* [2]*The Rolf Luft Center for Diabetes Research, Department of Molecular Medicine, Karolinska Institutet, Karolinska Hospital, Stockholm, Sweden.* [3]*Department of Pathology, Sahlgrenska University Hospital, Göteborg, Sweden.* [4]*Department of Molecular Physiology and Biophysics, Vanderbilt University School of Medicine, Nashville, Tennessee, USA. Correspondence should be addressed to N.-G.L. (e-mail: nils-goran.larsson@cmm.ki.se).*

© 2000 Nature America Inc. • http://genetics.nature.com

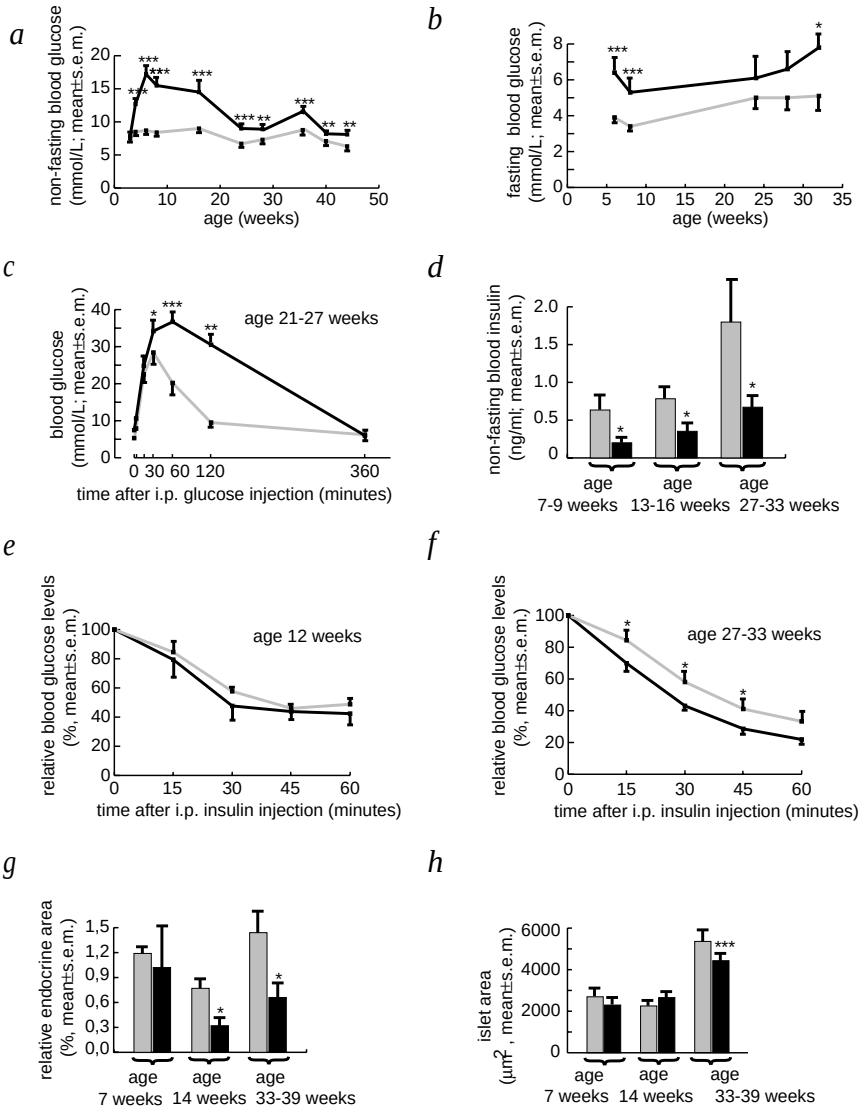

Fig. 2 Chemical blood analyses and morphometrical analyses in mutant mice (*Tfam*^{loxP}/*Tfam*^{loxP}, +/*RIP-cre*; black lines and bars) and littermate controls (*Tfam*^{loxP}/*Tfam*^{loxP}; grey lines and bars). ***a***, Non-fasting blood glucose concentrations at different ages. ***b***, Fasting blood glucose concentrations at different ages. ***c***, Glucose tolerance tests at 21–27 weeks of age. ***d***, Non-fasting blood insulin concentrations at different ages. ***e***, Insulin tolerance tests in 12-week mice. ***f***, Insulin tolerance tests at 27–33 weeks of age. ***g***, Relative pancreatic endocrine area determined by point-counting morphometry at different ages. ***h***, Absolute islet areas determined by image analysis at different ages. Values are presented as the mean±s.e.m. Unpaired (*a*,*b*,*d*–*h*) and paired (*c*) one sided *t*-tests were used to calculate the significance level (*P<0.05, **P<0.01 and ***P<0.001).

cristae in insulin-producing cells of mutant mice at 7–9 weeks (Fig. 1*b*). These morphological aberrations of mitochondria are typically found in tissues with severe respiratory chain dysfunction[8,9]. The mutant mice at 7 weeks thus had a highly efficient inactivation of mtDNA expression and, as a consequence, a severe respiratory chain deficiency in pancreatic β-cells.

The mutant mice developed diabetes (Fig. 2*a*–*c*) with decreased blood insulin concentrations (Fig. 2*d*) from the age of approximately 5 weeks. Insulin tolerance tests of mutant mice showed normal sensitivity at 12 weeks (Fig. 2*e*) and increased insulin sensitivity at 27–33 weeks (Fig. 2*f*).

We documented loss of β-cell mass over time in the mutant mice. Histochemical analyses of islet cell composition demonstrated a normal distribution of endocrine cells in mutant mice at 7 weeks (Fig. 3). The insulin-producing cells were evenly distributed and the glucagon- and somatostatin-producing cells were located peripherally in the islets. The cell type composition of islets of 39-week mutant mice showed an extensive loss of insulin-producing cells (Fig. 3). In addition, there was a relative increase of glucagon- and somatostatin-producing cells and many of these cells had an abnormal central location in the islets (Fig. 3). We also determined the ratio of pancreatic endocrine and exocrine tissue by point counting morphometry in mutant mice and found normal ratios at 7 weeks and reduced ratios at 14 and 33–39 weeks (Fig. 2*g*). Next, we measured mean islet areas by image analysis in mutant mice and found normal areas at 7 and 14 weeks, and reduced areas at 33–39 weeks (Fig. 2*h*).

Consistent with the absence of detectable *Tfam*$^{-}$ alleles in pancreas of older mutant mice, we observed normal COX activity in islets of 14–39-week mutant mice and normally appearing mitochondria on electron micrographs of β-cells of 29–33-week mutant mice (data not shown). We detected abundant expression of *cre* recombinase by immunofluorescence staining of islets from 7-week mutant mice, whereas *cre* recombinase was not expressed at all or in very few islet cells in 22–25-week mutant mice (data not shown). These findings further support the conclusion that the mutant β-cells were lost with time. We studied pancreatic tissue sections and found no evidence for increased apoptosis (<1% TUNEL reactive islet cells) or islet inflammation in mutant mice compared with controls at the age of 7 weeks. Patients with mitochondrial diabetes have a very similar phenotype with reduced β-cell mass without evidence of insulitis or apoptosis[13,14].

Older mutant mice were diabetic (Fig. 2*a*–*c*) with reduced β-cell mass (Figs 2*g*,*h* and 3), whereas younger mutant mice were diabetic (Fig. 2*a*–*c*) with normal β-cell mass (Figs 2*g*,*h* and 3). These findings suggested impaired β-cell stimulus–secretion coupling at younger ages. We therefore performed physiological *in vitro* studies of isolated islets from 7–8-week mutant mice. The β-cell stimulus–secretion coupling is initiated by glucose uptake and metabolism resulting in increased cytosolic ATP/ADP ratios, closure of ATP-dependent K^+-channels, depolarization of the plasma membrane, opening of voltage dependent L-type Ca^{2+}-channels, an increase in cytoplasmic free Ca^{2+} concentration $[Ca^{2+}]_i$ and exocytosis of insulin-containing secretory granules[15]. We measured a decreased hyper-

© 2000 Nature America Inc. • http://genetics.nature.com

© 2000 Nature America Inc. • http://genetics.nature.com

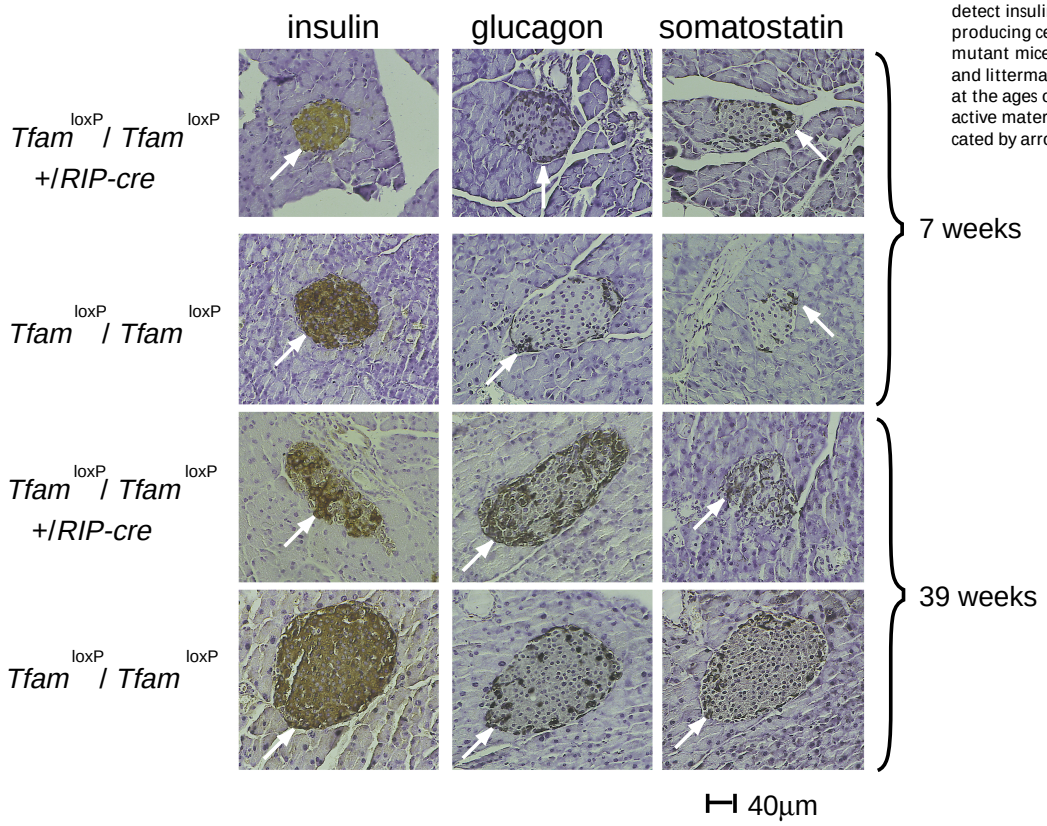

Fig. 3 Immunohistochemical analyses to detect insulin, glucagon and somatostatin producing cells in pancreatic sections from mutant mice (*Tfam*^{loxP}/*Tfam*^{loxP}, +/*RIP-cre*) and littermate controls (*Tfam*^{loxP}/*Tfam*^{loxP}) at the ages of 7 and 39 weeks. Immunoreactive material appears brown and is indicated by arrows. Bar, 40 μm.

polarization of the mitochondrial membrane potential in response to glucose in islets of mutant mice (Fig. 4*a*,*b*) at the ages of 7–8 weeks, consistent with a respiratory chain deficiency.

Ca^{2+} is the main trigger of insulin exocytosis[15]. We therefore monitored $[Ca^{2+}]_i$ after glucose stimulation of mutant (Fig. 4*d*) and control islets (Fig. 4*c*) at 7–8 weeks. There was a decreased $[Ca^{2+}]_i$ rise and an almost complete absence of the fast $[Ca^{2+}]_i$ oscillations (10–20 s) in islets of mutant mice (Fig. 4*d*). When islets of mutant mice and controls were exposed to K^+, which depolarizes the plasma membrane, both had similar patterns of $[Ca^{2+}]_i$ increase (Fig. 4*c*,*d*). It is thus possible to raise $[Ca^{2+}]_i$ in the mutant mice after depolarization of the plasma membrane by a mechanism independent of glucose metabolism.

Next, we studied the kinetics of glucose-induced insulin release by performing perifusions of islets isolated at the ages of 7–8 weeks. The insulin release was reduced in mutant islets (Fig. 5*a*), although the total insulin content was similar in mutant and control islets (Fig. 5*b*). This finding is in agreement with the reported decrease of glucose-stimulated insulin secretion in mitochondrial diabetes patients[5,16] and mtDNA-depleted β-cell lines[17,18].

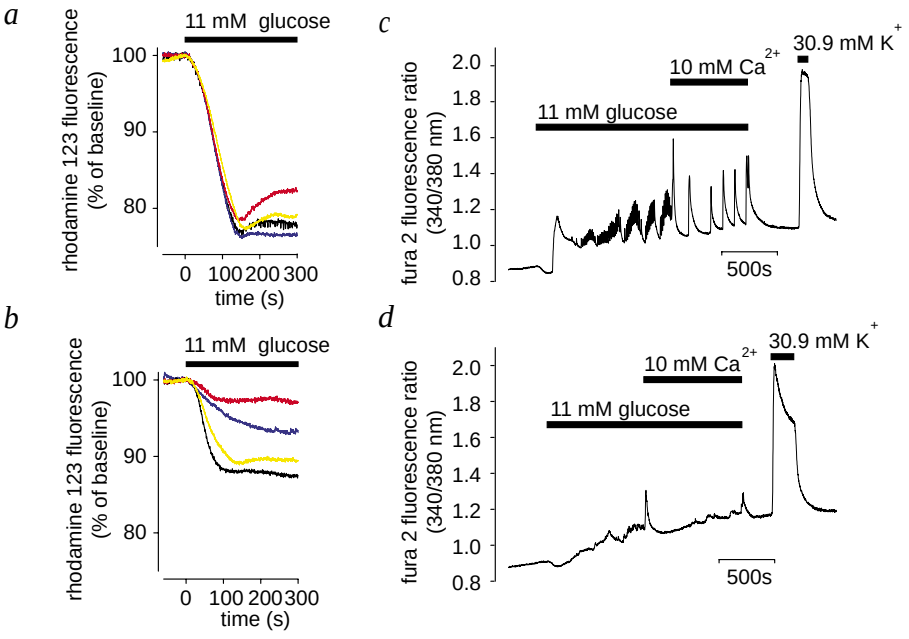

Fig. 4 Measurements of mitochondrial membrane potential and $[Ca^{2+}]_i$ in response to glucose in islets of mutant mice (*Tfam*^{loxP}/*Tfam*^{loxP}, +/*RIP-cre*) and controls (*Tfam*^{loxP}/*Tfam*^{loxP}) at 7–8 weeks. Measurement of the rhodamine 123 fluorescence (which decreases when the mitochondrial membrane polarizes) in controls (***a***) and mutants (***b***). The different colours indicate separate experiments carried out on single islets from mutant/control littermate pairs. The basal concentration of glucose was 3 mM. The signal was normalized to 100% just before raising the glucose concentration. $[Ca^{2+}]_i$ responses in islets of a control (***c***) and a mutant (***d***) mouse. Higher fura-2 fluorescence ratio indicates higher $[Ca^{2+}]_i$. The basal concentration of glucose was 3 mM. Extracellular Ca^{2+} and K^+ was changed to the final concentration as indicated in the panels. The response to K^+ shows the ability to increase $[Ca^{2+}]_i$ by directly depolarizing the cells and thereby induce opening of L-type Ca^{2+} channels.

© 2000 Nature America Inc. • http://genetics.nature.com

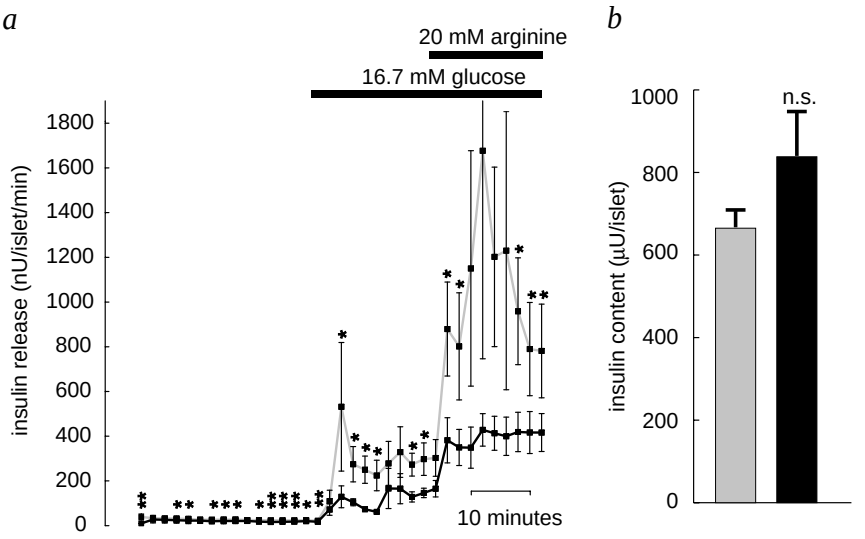

Fig. 5 Measurements of insulin release and insulin content in islets from mutant mice (*Tfam*^{loxP}/*Tfam*^{loxP}, +/*RIP-cre*; black line and bar) and controls (*Tfam*^{loxP}/*Tfam*^{loxP}; grey line and bar) at the ages of 7–8 weeks. Values are expressed as mean±s.e.m. ***a***, Measurements of insulin release from perifused islets. The basal glucose concentration was 3 mM and no arginine was present. The glucose concentration was increased and arginine was added as indicated in the panel. Arginine was used to define the total releasable pool of insulin. One sided paired *t*-tests were used to calculate the significance levels (**P*<0.05 and ***P*<0.01). ***b***, Mean insulin content in isolated and size-matched islets. Two-sided paired *t*-test was used to calculate the significance level (n.s., not significant).

The mutant mice were diabetic with impaired insulin secretion (Fig. 2*a*–*d*) and had normal or even increased insulin sensitivity (Fig. 2*e*,*f*). It is thus probable that the β-cell dysfunction was the principal determinant of the diabetic phenotype, as supported by the results from *in vitro* studies of isolated mutant islets. The low concentration of the *Tfam*-knockout allele in the brain may have no effect at all or may perhaps modify the diabetic phenotype by, for example, affecting central regulation of appetite or body weight.

The finding of a mosaic pattern with normally appearing β-cells (Fig. 3), lacking *cre* expression, in older mutant mice suggested that some β-cells had escaped recombination. There was an increase of mean islet area (Fig. 2*h*) and relative endocrine area (Fig. 2*g*) in both mutant mice and controls between the ages of 14 and 33–39 weeks, suggesting a physiological increase in β-cell mass during this period. The observed expansion of functional β-cells, together with the increased peripheral insulin sensitivity (Fig. 2*e*,*f*), may explain the less-pronounced elevation of blood glucose in mutant mice older than 20 weeks (Fig. 2*a*,*b*).

Patients with mitochondrial diabetes harbour point mutations or deletions affecting tRNA genes of mtDNA (refs 2,13,14) and display heteroplasmy with high concentrations of mutated mtDNA in islets[13,14]. The observed mosaic cell loss in human mitochondrial diabetes[13,14] is probably explained by varying mutant load in different β-cells and loss of respiratory chain deficient β-cells with high concentrations of mutated mtDNA. In accordance with this hypothesis, we observed that the respiratory chain deficient β-cells were lost in older mutant mice and the remaining β-cells all had normal respiratory chain function as determined by enzyme histochemistry.

The diabetic mice described here reproduce important pathophysiological features of mitochondrial diabetes and identify two phases in the progression of this disease; initially the mutant β-cells displayed impaired stimulus–secretion coupling, later followed by β-cell loss. This animal model provides genetic evidence for a critical role of the respiratory chain in normal glucose-induced insulin secretion and provides an important tool for further investigations of pathogenesis and treatment of mitochondrial diabetes.

Methods

Matings to disrupt *Tfam* in pancreatic β-cells. We mated *Tfam*^{loxP}/*Tfam*^{loxP} mice of mixed genetic background with +/*RIP-cre* mice. We identified double heterozygous offspring (+/*Tfam*^{loxP}, +/*RIP-cre*) from this first cross and mated them with *Tfam*^{loxP}/*Tfam*^{loxP} mice to obtain the *Tfam*^{loxP}/*Tfam*^{loxP}, +/*RIP-cre* mice carrying the tissue-specific disruption of *Tfam*. This latter mating produced normal litter sizes (mean litter size=8.9; n=577) and we recovered the different genotypes at the expected frequencies of ~25% each (*Tfam*^{loxP}/*Tfam*^{loxP}, +/*RIP-cre* (21%), +/*Tfam*^{loxP}, +/*RIP-cre* (27%), *Tfam*^{loxP}/*Tfam*^{loxP} (26%) and +/Tfam^{loxP} (26%)). We performed statistical analysis with the χ^2 test and found no significant difference between the expected and observed genotype frequencies (data not shown).

PCR genotyping. We determined the *Tfam* genotype and detected the *cre* transgene by PCR as described[8,9]. We performed PCR genotyping of several tissues from mutant mice (*Tfam*^{loxP}/*Tfam*^{loxP}, +/*RIP-cre*) at 7–9 weeks (number of mutant mice, n_{KO}=6), 14 weeks (n_{KO}=4) and 27–39 weeks (n_{KO}=4).

Histological and morphometrical analyses. We determined COX and SDH activities[8,9] by enzyme histochemical double staining of cryostat sections from pancreas obtained at the ages of 7 weeks (n_{KO}=3; littermate *Tfam*^{loxP}/*Tfam*^{loxP} controls, n_C=2) and 14–39 weeks (n_{KO}=5, n_C=4). We carried out morphological and morphometrical analyses on serial sections (4 μm) obtained from formaldehyde-fixed paraffin-embedded specimens taken from different regions of the pancreas. We studied morphology and cell type composition of islets at the ages of 7 weeks (n_{KO}=3, n_C=2) and 39 weeks (n_{KO}=3, n_C=2) by staining sections with haematoxylin and eosin and with an indirect immunoperoxidase technique using guinea pig anti-insulin (Dako), rabbit anti-somatostatin (Dako) or rabbit anti-glucagon antibodies (Dako) followed by a secondary antibody consisting of goat anti-rabbit immunoglobulin conjugated to a peroxidase labelled dextran polymer (Dako, EnVision+). We determined the relative endocrine areas at the ages of 7 weeks (n_{KO}=3, n_C=2), 14 weeks (n_{KO}=3, n_C=3) and 33–39 weeks (n_{KO}=4, n_C=3) by conventional point counting morphometry[19] using a grid mounted in the ocular eyepiece of the microscope (Leitz). The whole surface of each section was investigated at 100-fold magnification and the number of intercepts falling on endocrine and exocrine cells were counted at 5 different levels of the pancreas. We divided the number of intercepts falling on endocrine cells by intercepts falling on exocrine cells and expressed the results as a percentage. The total number of intercepts examined in each animal varied between 726 and 4,215. We excluded blood vessels, nerves, fat and connective tissue from the counting. We determined islet areas at the ages of 7 weeks (n_{KO}=3, n_C=2), 14 weeks (n_{KO}=3, n_C=3) and 33–39 weeks (n_{KO}=4, n_C=3) by measurements with an image analysis program (National Institutes of Health Image 1.41; http://rsb.info.nih.gov/nih-image). Immunofluorescence to detect the *cre* protein was performed as described[10].

In situ hybridization and electron microscopy. We determined concentrations of mtDNA by *in situ* hybridization[8] of cryostat sections from pancreas at the age of 7 weeks (n_{KO}=3, n_C=2) and performed electron microscopy of pancreas at 7–9 weeks (n_{KO}=3, n_C=3) and 29–33 weeks (n_{KO}=4, n_C=4).

Glucose and insulin measurements. We determined blood glucose concentrations from tail vein blood by using an automatic glucometer (HemoCue AB). We measured non-fasting blood glucose concentrations in the morning between 10 and 12 AM at regular intervals between the ages of 4 and 45 weeks (n_{KO}=5–18, n_C=3–50). We measured fasting blood glucose concentrations in the morning after 14–16 h of overnight starvation

© 2000 Nature America Inc. • http://genetics.nature.com

© 2000 Nature America Inc. • http://genetics.nature.com

at regular intervals between the ages of 5–33 weeks (n_{KO}=6–12, n_C=4–22). We determined non-fasting blood insulin concentrations at the ages of 7–9 weeks (n_{KO}=7, n_C=6), 13–16 weeks (n_{KO}=7, n_C=7) and 27–33 weeks (n_{KO}=9, n_C=7) by collecting blood from the tail vein in heparinized tubes (Sarstedt). The samples were immediately centrifuged and the plasma was stored at –20 °C. We measured insulin with a rat insulin ELISA kit using a rat insulin standard (Crystal Chem). Insulin concentrations were calculated using the Microplate Manager 4.0 program (Biorad).

Glucose and insulin tolerance tests. We performed insulin tolerance tests at the ages of 12 weeks (n_{KO}=7, n_C=5) and 27–33 weeks (n_{KO}=9, n_C=9). We subjected mice to fasting overnight for 14–16 h and then injected them intraperitoneally with insulin (0.5 U/kg body weight in the 12-week mice and 0.75 U/kg body weight in the 27–33-week mice). We observed that normal 12-week mice were much more sensitive to insulin than normal 27–33-week mice and we therefore administered different insulin doses depending on the age of the mice. We found no difference in absolute blood glucose concentrations between 27–33-week controls and mutant mice at 15, 30, 45 and 60 min after insulin injection. We performed glucose tolerance tests at the ages of 5–20 weeks (n_{KO}=6, n_C=6) and 21–27 weeks (n_{KO}=9, n_C=9). We subjected mice to fasting overnight for 14–16 h, injected them intraperitoneally with glucose (2 g/kg body weight) and determined blood glucose concentrations with an automatic glucometer (HemoCue AB).

Islet isolation. We used buffer A (25 mM HEPES, pH 7.4, 125 mM NaCl, 5.9 mM KCl, 2.56 mM $CaCl_2$, 1.2 mM $MgCl_2$ and 1 mg/ml bovine serum albumin) with 3 mM glucose as medium for isolation of islets from pancreas with the collagenase technique, as described[20]. We cultured islets in RPMI 1640 culture medium containing 11 mM glucose, supplemented with 10% fetal bovine serum, 2 mM L-glutamine, 50 IU/ml penicillin and 50 µg/ml streptomycin (Gibco BRL).

Mitochondrial membrane potential in intact islets. We loaded islets with rhodamine 123 (rh123) by incubation for 10 min with 32 µM rh123 (Molecular Probes) at 37 °C in buffer A with 3 mM glucose. We did the measurements essentially as for $[Ca^{2+}]_i$ in intact islets. The excitation was set to 500 nm and the emission was collected at 515–565 nm. We analysed a total of 4 islets from 4 mutant mice and 4 islets from their 4 littermate controls at 7–8 weeks.

$[Ca^{2+}]_i$ in intact islets. We loaded islets with fura-2 by incubating them for 60 min with fura-2/AM (2 µM) and 0.01% pluronic F-127 (Molecular Probes) at 37 °C in buffer A with glucose (3 mM). We performed measurements with a SPEX fluorolog-2 system (Spex Industries) connected to an Zeiss Axiovert 135TV inverted microscope with the islets situated in a custom built open perifusion chamber with a flow rate of 0.15 ml/min at 37 °C. We used the Zeiss Fluar ×40/1.30 oil lens. We set the excitation to 340 and 380 nm, and the emission was collected at 500–530 nm. We analysed a total of 4 islets from 3 mutant mice and 4 islets from their 3 littermate controls at the ages of 7–8 weeks.

Insulin secretion and insulin content. We cultured islets from 7–8-week mice overnight and then loaded them into a 0.5-ml perifusion column filled with Bio-Gel P-4 polyacrylamide beads[21] (Biorad). We set the perifusion rate at ~0.15 ml/min and collected samples every 2 min. We determined insulin secretion with RIA using a rat insulin standard. We performed a total of 4 experiments with mutant and control islets and for each experiment we isolated 70–120 islets from 2 to 4 mice. We determined the islet insulin content by RIA of acid ethanol extracts of 60 islets from 8 mutant mice and 60 islets from eight controls at the age of 8 weeks.

Acknowledgements

N.-G.L. is supported by grants from the Swedish Medical Research Council, Swedish Heart and Lung Foundation, Petrus och Augusta Hedlunds Stiftelse, Emil och Vera Cornells Stiftelse, Funds of Karolinska Institutet and Novo Nordisk Pharma AB. C.G. is supported by a grant from the Swedish Diabetes Association, The Swedish Society of Medicine and Knut and Alice Wallenberg Stiftelse. J.S. is supported by a stipend from the Roche Research Foundation. A.O. is supported by a grant from the Swedish Medical Research Council. P.-O.B. is supported by grants from the Swedish Medical Research Council, the Swedish Diabetes Association, the Nordic Insulin Foundation Committee, Funds of Karolinska Institutet, Berth von Kantzows Foundation, Juvenile Diabetes Foundation International, the Swedish Society for Medical Research and the Novo Nordisk Foundation.

Received 6 March; accepted 10 August 2000.

1. Wallace, D.C. Mitochondrial diseases in man and mouse. *Science* **283**, 1482–1488 (1999).
2. Larsson, N.G. & Clayton, D.A. Molecular genetic aspects of human mitochondrial disorders. *Annu. Rev. Genet.* **29**, 151–178 (1995).
3. Larsson, N.G. & Luft, R. Revolution in mitochondrial medicine. *FEBS Lett.* **455**, 199–202 (1999).
4. Graff, C., Clayton, D.A. & Larsson, N.G. Mitochondrial medicine—recent advances. *J. Int. Med.* **246**, 11–23 (1999).
5. Kadowaki, T. *et al.* A subtype of diabetes mellitus associated with a mutation of mitochondrial DNA. *N. Engl. J. Med.* **330**, 962–968 (1994).
6. Majamaa, K. *et al.* Epidemiology of A3243G, the mutation for mitochondrial encephalomyopathy, lactic acidosis, and strokelike episodes: prevalence of the mutation in an adult population. *Am. J. Hum. Genet.* **63**, 447–454 (1998).
7. Parisi, M.A. & Clayton, D.A. Similarity of human mitochondrial transcription factor 1 to high mobility group proteins. *Science* **252**, 965–969 (1991).
8. Larsson, N.G. *et al.* Mitochondrial transcription factor A is necessary for mtDNA maintenance and embryogenesis in mice. *Nature Genet.* **18,** 231–236 (1998).
9. Wang, J. *et al.* Dilated cardiomyopathy and atrioventricular conduction blocks induced by heart-specific inactivation of mitochondrial DNA gene expression. *Nature Genet.* **21**, 133–137 (1999).
10. Postic, C. *et al.* Dual roles for glucokinase in glucose homeostasis as determined by liver and pancreatic β cell-specific gene knock-outs using Cre recombinase. *J. Biol. Chem.* **274**, 305–315 (1999).
11. Kulkarni, R.N. *et al.* Tissue-specific knockout of the insulin receptor in pancreatic beta cells creates an insulin secretory defect similar to that in type 2 diabetes. *Cell* **96**, 329–339 (1999).
12. Gannon, M., Postic, C., Shiota, C., Wright, C.V.E. & Magnuson, M.A. Cre-mediated recombination driven by rat insulin promoter in embryonic and adult mouse pancreas. *Genesis* **26**, 139–141 (2000).
13. Kobayashi, T. *et al.* In situ characterization of islets in diabetes with a mitochondrial DNA mutation at nucleotide position 3243. *Diabetes* **46**, 1567–1571 (1997).
14. Otabe, S. *et al.* Molecular and histological evaluation of pancreata from patients with a mitochondrial gene mutation associated with impaired insulin secretion. *Biochem. Biophys. Res. Commun.* **259**, 149–156 (1999).
15. Berggren, P.O. & Larsson, O. Ca^{2+} and pancreatic B-cell function. *Biochem. Soc. Trans.* **22**, 12–18 (1994).
16. Velho, G. *et al.* Clinical phenotypes, insulin secretion, and insulin sensitivity in kindreds with maternally inherited diabetes and deafness due to mitochondrial $tRNA^{Leu(UUR)}$ gene mutation. *Diabetes* **45**, 478–487 (1996).
17. Soejima, A. *et al.* Mitochondrial DNA is required for regulation of glucose-stimulated insulin secretion in a mouse pancreatic beta cell line, MIN6. *J. Biol. Chem.* **271**, 26194–26199 (1996).
18. Kennedy, E.D., Maechler, P. & Wollheim, C.B. Effects of depletion of mitochondrial DNA in metabolism secretion coupling in INS-1 cells. *Diabetes* **47**, 374–380 (1998).
19. Guenifi, A., Abdel-Halim, S.M., Hoog, A., Falkmer, S. & Östenson, C.G. Preserved β-cell density in the endocrine pancreas of young, spontaneously diabetic Goto-Kakizaki (GK) rats. *Pancreas* **10**, 148–153 (1995).
20. Lacy, P.E. & Kostianowsky, M.K. Method for the isolation of intact islets of Langerhans from the rat pancreas. *Diabetes* **16**, 35–39 (1967).
21. Kanatsuna, T., Lernmark, A., Rubenstein, A.H. & Steiner, D.F. Block in insulin release from column-perifused pancreatic β-cells induced by islet cell surface antibodies and complement. *Diabetes* **30**, 231–234 (1981).

© 2000 Nature America Inc. • http://genetics.nature.com